On the importance of the reference data: Uncertainty partitioning of bias-adjusted climate simulations over eastern Canada

Juliette Lavoie, Louis-Phillipe Caron, Travis Logan, Stephen Sobie, Richard Turcotte, Edouard Mailhot & Jasmine Pelletier-Dumont

2025

Pacific Climate Impacts Consortium (PCIC)

PCIC Publications

Original citation:
Lavoie, J., Caron, L., Logan, T., Sobie, S., Turcotte, R., Edouard, M., & Pelletier Dumont, J. (2025). On the importance of the reference data: Uncertainty partitioning of bias-adjusted climate simulations over eastern Canada. Climate Services, 40, 100619. https://doi.org/10.1016/j.cliser.2025.100619

Climate Services 40 (2025) 100619

Contents lists available at ScienceDirect

Climate Services

journal homepage: www.elsevier.com/locate/cliser

Original research article

On the importance of the reference data: Uncertainty partitioning of bias-adjusted climate simulations over eastern Canada

Juliette Lavoie [a,*], Louis-Philippe Caron [a], Travis Logan [a], Stephen Sobie [b], Richard Turcotte [c], Edouard Mailhot [c], Jasmine Pelletier-Dumont [c]

[a] *Ouranos, 550 Sherbrooke W., Montreal, H3A 1B9, QC, Canada*
[b] *Pacific Climate Impacts Consortium, University of Victoria, 2489 Sinclair Road, University of Victoria, Victoria, V8W 2Y2, British Columbia, Canada*
[c] *Direction principale de l'expertise hydrique, Ministère de l'Environnement, de la Lutte contre les changements climatiques, de la Faune et des Parcs, 675, boul. René-Lévesque Est, Quebec, V8W 2Y2, Quebec, Canada*

HIGHLIGHTS

- The uncertainty of bias-adjusted climate simulations is divided between 5 dimensions.
- Observational reference is often an important share of the uncertainty.
- The choice of reference can lead to different decisions in climate change adaptation.

ARTICLE INFO

Keywords:
Climate data adaptation
Bias-correction
Climate simulations
Uncertainty
Observational reference
Reanalysis

ABSTRACT

Bias-adjusted climate simulations are increasingly disseminated through online platforms to support adaptation actions. However, there is no consensus on an operational framework to choose what to include in these "decision-ready" ensembles and for communicating the related uncertainty. In this paper, we use a systematic approach to assess the uncertainty related to bias-adjusted climate simulations across five dimensions: internal variability, greenhouse gases scenario, global climate model, observational reference and bias-adjustment method. We calculate the fraction of uncertainty associated with each dimension for precipitation-based, temperature-based and multivariate indicators over eastern Canada and focus particularly on three locations: Montréal, Gaspé and Kawawachikamach. The results show that the uncertainty associated with the reference dataset can be very large and in some instances can become the first or second largest source of uncertainty. Using simple examples, we show that the resulting differences could lead to different conclusions with respect to some adaptation solutions or possibly create confusion with users. These results raise questions on the robustness of climate projections distributed through these web platforms and the ethical responsibility of data providers to adequately evaluate and communicate the underlying uncertainty.

Practical implications

Bias-adjusted climate simulations are shared online to help people make decisions about adapting to climate change. However, there is no standard way to create or share these simulations, especially when it comes to explaining their uncertainty. This study looks at the uncertainty in these simulations by examining five key factors: natural climate variability (how much the indicators change year-to-year), future socioeconomic scenarios (how much greenhouse gases will be released in the atmosphere by humans), global climate models (physical models of the Earth), reference data used (observation data assumed to represent the truth), and the methods for adjusting biases (mathematical algorithms to bring the output of the model closer to the reference). The researchers focused on precipitation, temperature, and combined indicators for eastern Canada, with special attention to Montréal, Gaspé, and Kawawachikamach. They found that the choice of reference data can cause the value of the indicators calculated from bias-adjusted climate simulations to change widely, sometimes being the largest or second-largest source of uncertainty. They also showed how these differences could lead to conflicting conclusions about adaptation strategies. This study should raise a flag with climate services providers to better consider how to include the uncertainty reference data in their bias-adjusted climate simulations ensemble.

* Corresponding author.
E-mail address: lavoie.juliette@ouranos.ca (J. Lavoie).

https://doi.org/10.1016/j.cliser.2025.100619
Received 14 February 2025; Received in revised form 10 October 2025; Accepted 10 October 2025
Available online 29 October 2025

1. Introduction

There is a growing demand for climate information. This demand is fuelled by a growing awareness of the impacts of anthropogenic climate change, but also by the need to inform national adaptation strategies as countries aim to reduce the risks associated with a changing climate. To facilitate the implementation of adaptation strategies, climate information is often made available through web portals developed by government agencies or boundary organizations, such as regional climate service providers.[1] Future projected changes are largely based on simulations produced within the context of the Climate Model Intercomparison Project (CMIP; Eyring et al., 2016). However, owing to the coarse resolution and inherent biases present in the initial model outputs, it is frequently deemed necessary to perform an additional step of downscaling and bias adjustment. Downscaling can be done through the use of regional climate models (RCMs), through coordinated exercises like CORDEX (Mearns et al., 2017) or the use of in-house RCMs, but is also often performed through statistical downscaling or simple bias adjustment. Several studies have made recommendations on how to properly apply a statistical downscaling and a bias adjustment (Cannon et al., 2015; Pierce et al., 2015; Chadwick et al., 2023) or how to evaluate such methods (Maraun et al., 2015; Sun et al., 2020). However, these evaluation frameworks are not always implemented by the community when documenting their choice of method. Moreover, there exists no agreed upon operational framework for the complete production and documentation of these "decision-ready" ensembles. Many assumptions and choices made in the construction of these datasets have the potential to substantially alter the results and, ultimately, impact decision outcomes. The transparency and understanding of these choices can vary greatly for users: some choices can be readily available, some might require a deeper understanding of the field and access to scientific journals while others can be completely hidden. The limited capacity of users to comprehend these kinds of constraints fosters overconfidence in the robustness of climate information and can potentially produce contradictions (real or perceived) between datasets.

Methodological choices made by scientists in the construction of these ensembles include the selection of the future greenhouse gases scenarios, the selection of the global climate models and the downscaling methodology. Lafferty and Sriver (2023), hereafter referred to as LS23, have shown that the latter can be an important source of uncertainty, sometimes more important than the other two. However, embedded (and hidden) in a statistical downscaling approach is the selection of the observational reference used for the bias adjustment. Typically, the reference dataset is selected from available observational products, such as reanalysis or gridded observations, which possess the necessary spatial and temporal properties for the application. This choice can be made based on various factors, such as perceived overall quality or ease of access, but the motivation behind the selection is rarely communicated to users. However, it is well known that there can be significant differences between observational datasets, particularly for precipitation (Gebrechorkos et al., 2023; Iizumi et al., 2017; Rastogi et al., 2022; Gampe et al., 2019; Wootten et al., 2021). The impact of this selection and the uncertainty that it introduces in the statistically downscaled ensemble is often, if not always, overlooked. LS23 showed that a large share of the uncertainty associated with the bias-adjusted ensemble could be linked to the downscaling procedure and provided qualitative evidence that, in many cases, the uncertainty was originating from disagreements in the historical record and not necessarily in the statistical procedure per se. However, their methodology did not allow them to distinguish between the two. Here, using a systematic approach instead of an ensemble of opportunity (as was done in LS23), we explore the share of uncertainty of a bias-adjusted ensemble along five dimensions: greenhouse gases scenario, global climate models, bias-adjustment methodology, observational reference and internal variability. This allows us to isolate the share of uncertainty linked to the reference dataset and thus better understand the impact of neglecting this factor in the creation of a bias-adjusted ensemble.

In Section 2, we describe the various datasets (models, scenarios, observational references and bias-adjustment methodologies) included in this study, as well as the mathematical framework for the partition of uncertainties. In Section 3, we show results for three specific locations as well as for eastern Canada more broadly while in Section 4, we discuss the results in a decision-making context. We conclude in Section 5.

2. Data and methods

2.1. Datasets

The datasets in this study combine 4 greenhouse gases scenarios, 11 global climate models, 4 observational references and 4 bias-adjustment methods to create a complete ensemble. Fig. 1 shows the data available. The domain of the study is centred on eastern Canada (55–83°W, 42–63°N). The domain and size of the datasets was informed by computational resources constraints.

The selection of bias-adjustment methods and observational references used in this paper were made to reflect important climate and hydrological portals available in Quebec and Canada. For the Canadian-wide climate portal www.climatedata.ca, the Pacific Climate Impacts Consortium (PCIC) created CanDCS-M6 (using the `MBCn` method and the *PCICBlend* reference; Sobie et al., 2024) and CanDCS-U6 (using the `BCCAQv2` method and a reference dataset similar to *PCICBlend*, *NRCANmet v2012*). For the Quebec-specific climate portal Portraits climatiques,[2] Ouranos created ESPO-G6-R2 v1.0 (using the `DQM` method and the *CaSR v2.1* reference; Lavoie et al., 2024a) . A similar dataset, ESPO-G6-E5L v1.0, (using the `DQM` method and the *ERA5-Land* reference) is available on Ouranos' data distribution server PAVICS (Power Analytics and Visualization for Climate Science). For the Hydroclimatic Atlas of Southern Quebec,[3] Ouranos developed the `DQM-EV` method in order to properly capture extremes in precipitation, which are very important for hydrological modelling of high water flows. Thus, the new datasets presented here were created around the techniques and data used in the production of these existing datasets.

First, we present an overview of the various observational references. These are being used as is, without any extra processing or correction.

1. Canadian Surface Reanalysis (*CaSR v2.1*): The Canadian reanalysis was created by Environment and Climate Change Canada (ECCC) using the Regional Deterministic Reforecast System (RDRS). Unlike other reanalysis products, it includes a final step that re-assimilates observed precipitation from the Canadian Precipitation Analysis System (CaPA) (Gasset et al., 2021).
2. The land component of the fifth generation of European ReAnalysis (*ERA5-Land*): This well-known global reanalysis was created by the European Centre for Medium-Range Weather Forecasts (ECMWF) (Copernicus Climate Change Service, 2019).
3. *PCICBlend*: This gridded observation dataset was constructed by the Pacific Climate Impacts Consortium (PCIC) by blending 3 station datasets: PCIC meteorology for Northwest North America (PNWNAmet) (Werner and Cannon, 2015), NRCANmet v2018 daily maximum and minimum temperatures (McKenney et al., 2011), and daily precipitation from NRCANmet-Adjusted (Wang

[1] portraits.ouranos.ca, climatedata.ca,atlas.globalchange.gov, www.climatechangeinaustralia.gov.au/en/projections-tools, www.nccs.admin.ch/nccs/en/home/climate-change-and-impacts/swiss-climate-change-scenarios/ch2018-web-atlas.html,

[2] portraits.ouranos.ca

[3] cehq.gouv.qc.ca/atlas-hydroclimatique/carte-indicateurs/index-en.htm

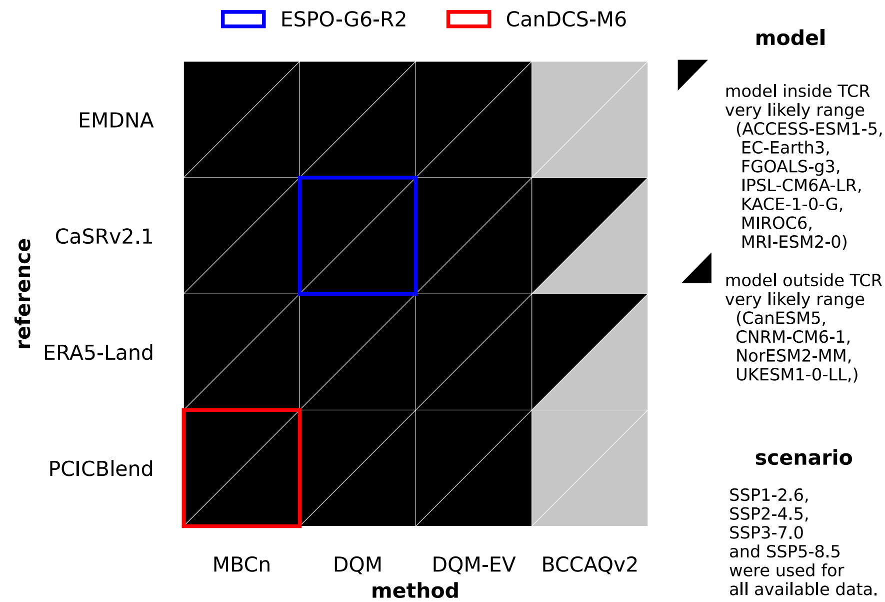

Fig. 1. Data included in the study. Black triangles means that this dataset exists, grey means that it is unavailable. Coloured contours indicate an official dataset presented on a provincial or national portal.

et al., 2017). We note however that PNWNAmet only covers the western part of North America and is not included in our domain.

4. Ensemble Meteorological Dataset for North America (*EMDNA*): This reconstruction combines outputs from three larger resolution reanalyses (ERA5, MERRA-2 and JRA-55) and the Serially Complete Dataset for North America (SCDNA) station data. It contains 100 members, but for this study only one member, constructed using optimal interpolation, is used. This reference is not currently used by any climate portal, but was included here to increase the number of reference datasets given that its resolution is similar to that of the other references (Tang et al., 2021).

Timeseries of the reference data at our three locations are shown in Figs. S1 to S4 and standard deviation between the different references are show in Figs. S5 to S7. It is important to keep in mind that these product are used as the ground truth in the bias-adjustment procedure, but they are not, in fact, direct observations or a perfect representation of reality and have some inherent biases.

The various bias-adjustment methods selected are:

1. Detrended Quantile Mapping (`DQM`): Based on the widely recognized family of univariate methods of quantile mapping, this methodology (Cannon et al., 2015) preserves the trend of the original timeseries. For this study, the adjustment was applied on a rolling 31-day window and, instead of directly adjusting the minimum daily temperature, we adjusted the maximum daily temperature and the diurnal range as a way to ensure that the maximum temperature remains higher than the minimum temperature. The method also includes a pre-processing step to adapt the frequency of simulated dry days to the observations. The complete method is described in Lavoie et al. (2024a).
2. Bias Correction/Constructed Analogues with Quantile Mapping Reordering (`BCCAQv2`): This is a univariate method that combines Bias Corrected Climate Imprint (BCCI; Hunter and Meentemeyer, 2005), Bias Corrected Constructed Analogs (BCCA; Maurer and Hidalgo, 2008)), and Quantile Delta Mapping (QDM; Cannon et al., 2015). Marginal distributions of variables are adjusted using BCCI and QDM, while information about large-scale patterns are obtained from spatial analogs using BCCA.
3. Detrended Quantile Mapping - Extreme Values (`DQM-EV`): This univariate method is similar to `DQM`. However, a special adjustment for extremes is applied to precipitation. The tail of the distribution is adjusted using a Generalized Pareto distribution. The method is described in Roy et al. (2024).
4. N-Dimensional Multivariate Bias Correction (`MBCn`): Inspired by an image processing algorithm, this method successively applies QDM to random orthogonal rotations of the data until the multivariate distribution matches the reference dataset. This is the only multivariate method. The method is described in Cannon (2018).

   We note that `DQM` and `DQM-EV` return the same result for temperature, since the correction of extremes is only applied to precipitation in `DQM-EV`. Hence, there is effectively only three different methodologies for temperature. Obviously, these are not the only methods available for bias adjustment. Notable other examples include scaled distribution mapping (SDM) (Switanek et al., 2017) and the multivariate method two-stage quantile mapping (TSQM) (Guo et al., 2019). However, in the study, to ensure the applicability of the methods, we decided to restrict our choices to methods that are used operationally in Canada. This choice might affect the results of this study, as considering additional methodologies could increase the share of the variance associated with the correction method.

Given the constraints of limited computational resources and data availability, 11 models were chosen for this study (see Table 1). They were selected to span the full range of climate sensitivity. While this approach ensures a comprehensive representation of uncertainty across all variables, it may also amplify temperature-related uncertainty due to the inclusion of high-sensitivity models. To address this concern, known as the “hot model problem” (Hausfather et al., 2022), some climate services platforms, such as the Portraits climatiques by Ouranos, exclude models whose transient climate response (TCR) falls outside the IPCC AR6’s likely or very likely range (Forster and Storelvmo, 2023). As this method has not yet reached consensus among the community, in this study, we opted to include a carefully balanced subset of models, including some with a high climate sensitivity, without over-representing them. On top of the complete ensemble shown in Section 3, results with a constrained ensemble, including only models in the very likely TCR range, are available in the Supplemental Information (Figs. S8 to S10).

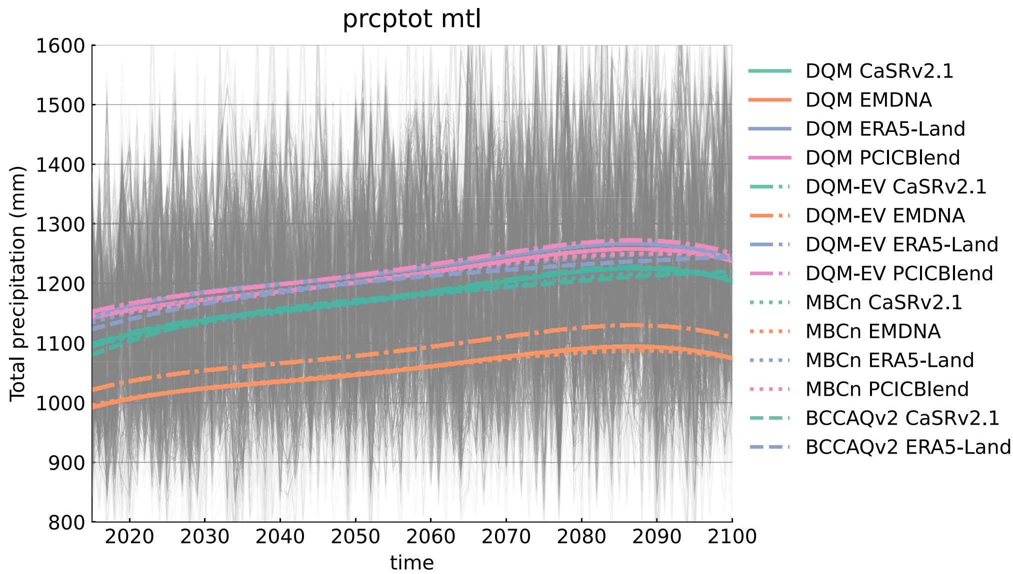

Fig. 2. Timeseries of annual total accumulated precipitation for Montréal. Grey lines show individual timeseries for each scenario, model, reference and method. The coloured lines show the forced responses for a given reference and method, averaged across models and scenarios.

Table 1
Models used in this study. For temperature-only indicators, only the models in the TCR very likely range, with a checkmark, were used.

Global climate model	Inside the TCR very likely range	Reference
ACCESS-ESM1–5	✓	Ziehn et al. (2019)
EC-Earth3	✓	EC-Earth Consortium (2019)
FGOALS-g3	✓	Li (2019)
IPSL-CM6A-LR	✓	Boucher et al. (2019)
KACE-1-0-G	✓	Byun et al. (2019)
MIROC6	✓	Shiogama et al. (2019)
MRI-ESM2–0	✓	Yukimoto et al. (2019)
CanESM5	X	Swart et al. (2019)
CNRM-CM6–1	X	Voldoire (2019)
NorESM2-MM	X	Bentsen et al. (2019)
UKESM1-0-LL	X	Good et al. (2019)

Note that the methods DQM and DQM-EV use EC-Earth3 r1i1p1f1 and KACE-1-0-G r1i1p1f1 while BCCAQv2 and MBCn use EC-Earth3 r4i1p1f1 and KACE-1-0-G r2i1p1f1 due to availability at the institutions who computed them. Also, the models outside of the TCR very likely range are not available for the BCCAQv2 method (see Fig. 1).

In CMIP6, the scenarios are called Shared Socioeconomic Pathways (SSP). The analysis is performed using all the tier 1 scenarios: a low (SSP1-2.6), a moderate (SSP2-4.5), a high (SSP3-7.0) and a very high (SSP5-8.5) emissions scenarios. Once again, this choice makes sure that we cover a very wide range of possibilities. We note that many studies have shown that not all scenarios are equally likely (Hausfather and Peters, 2020; Huard et al., 2022; Gillett, 2024). The middle two scenarios are recommended for most adaptation planning in the province of Quebec (Ouranos, 2023). Additional results with a constrained, more realistic, ensemble including only the scenarios SSP2-4.5 and SSP3-7.0, as well as a smaller set of models, are shown in the Supplemental Information (Figs. S8 to S10).

All bias-adjusted datasets included in the study have a similar resolution around 10 km. For figures based on individual grid points, the grid point closest to the coordinate is taken on the original grid. For figures with maps, all datasets were regridded on a common 0.1°x 0.1°grid. The common grid is masked if any reference is missing data over that grid point (e.g., over the sea).

Analysis and comparisons between the bias-adjusted datasets are performed using nine annual climate indicators (Table 2) that are derived from the daily simulations of minimum temperature, maximum temperature, and daily precipitation produced using each method and references. These derived indicators include both average and extreme quantities of precipitation and temperature, as well as two commonly used multivariate indicators.

2.2. Partitioning formulas

In this paper, we partition the uncertainty into five distinct dimensions: internal variability, scenario, model, observational reference and bias-adjustment method. The partitioning of the uncertainty is based on LS23 and Hawkins and Sutton (2009), wherein we first isolate the forced response by taking a 4th order polynomial of a yearly timeseries for a given climate indicator at a given location from 2015 to 2100. Fig. 2 shows an example of the forced response for total accumulated precipitation for each method and reference, averaged over the models and scenarios (colour), as well as for all the timeseries (light grey).

$$x(g,s,m,r,t) = \hat{x}(g,s,m,r,t) + \epsilon(g,s,m,r,t), \tag{1}$$

where $x_{g,s,m,r,t}$ is the original indicator timeseries based on global climate model (g), scenario (s), method (m), reference (r) and time (t), $\hat{x}$ is the forced response and ϵ is the residual.

The interannual variability (U_v) is calculated as the centred rolling 11-year variance of the residual ϵ, averaged over all four dimensions.

$$U_v(t) = \frac{1}{N}\sum_{g,s,m,r} \mathrm{var}_{(t-5,t+5)}\epsilon(g,s,m,r,t), \tag{2}$$

where N is the total number of datasets.

The scenario uncertainty is the variance over the scenario dimension of the mean over the other dimensions:

$$U_s(t) = \mathrm{var}_s\left[\frac{1}{N(s)}\sum_{g,m,r}\hat{x}(g,s,m,r,t)\right], \tag{3}$$

where $N(s)$ is the number of datasets (combining model, method and reference) available for a given scenario.

The model uncertainty is the weighted mean of the variance over the models.

Table 2
Climate Indicators used in this study.

Type	Short form	Description
Precipitation	**prcptot**	Annual total accumulated precipitation
	rx1day	Annual maximum daily precipitation
	r20mm	Total number of days with at least 20 mm of precipitation
	dry_days	Total number of days with less than 1 mm of precipitation
Temperature	**tg_mean**	Annual mean temperature
	tx_max	Annual maximum temperature
	tx_30	Total number of days with maximum temperature above 30 °C
Multivariate	**dlyfrzthw**	The number of days with a freeze-thaw cycle (where maximum daily temperature is above a 0 °C and minimum daily temperature is at or below 0 °C)
	solidprcptot	Total accumulated solid precipitation. Precipitation is considered solid when the average daily temperature is at or below 0 °C

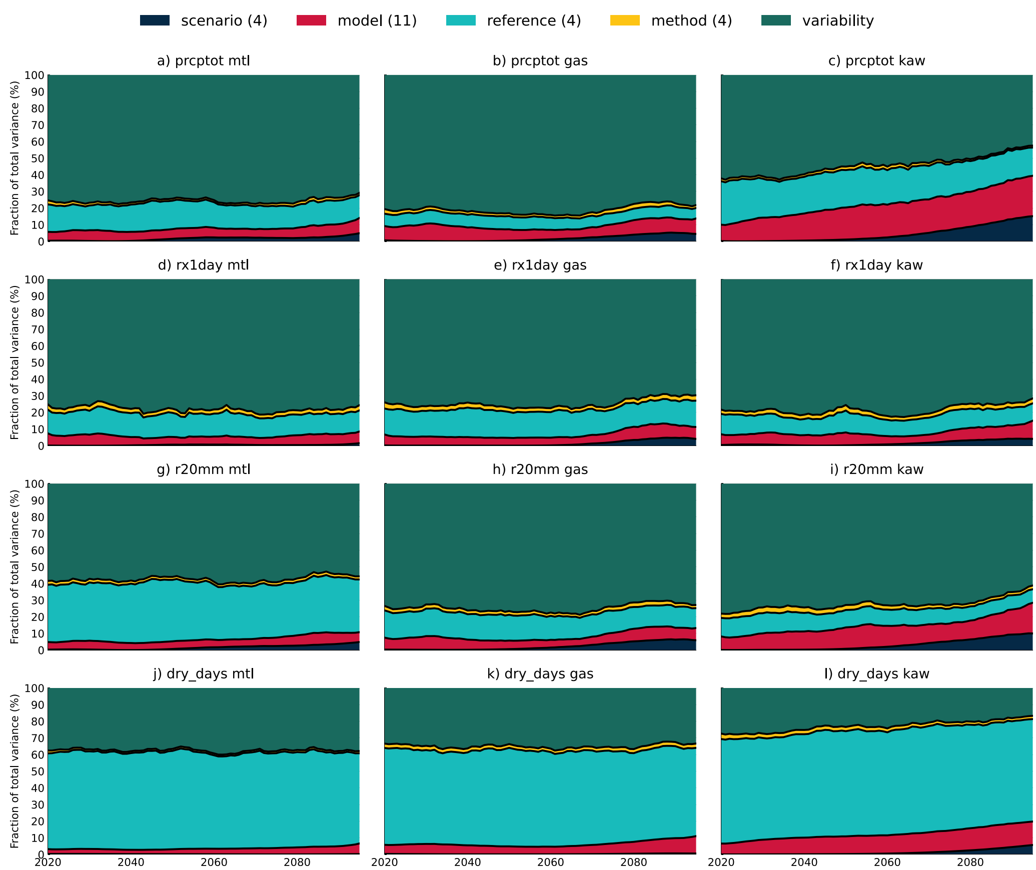

Fig. 3. Fraction of the total variance for precipitation indicators over Montréal (mtl), Gaspé (gas) and Kawawachikamach (kaw).

$$U_g(t) = \sum_{s,m,r} w_{s,m,r} \mathrm{var}_g \left[\hat{x}(g,s,m,r,t)\right], \tag{4}$$

where w are the weights,

$$w_{s,m,r} = \frac{g_{s,m,r}}{\sum_{s,m,r} g_{s,m,r}}, \tag{5}$$

where $g_{s,m,r}$ is the number of model available for a given scenario, method and reference.

The uncertainty associated with the bias-adjustment method is the weighted mean of the variance over the methods.

$$U_m(t) = \sum_{g,s,r} w_{g,s,r} \mathrm{var}_m[\hat{x}(g,s,m,r,t)], \tag{6}$$

where w are the weights,

$$w_{g,s,r} = \frac{m_{g,s,r}}{\sum_{g,s,r} m_{g,s,r}}, \tag{7}$$

where $m_{g,s,r}$ is the number of methods available for a given model, scenario, and reference.

The reference uncertainty is the weighted mean of the variance over the references.

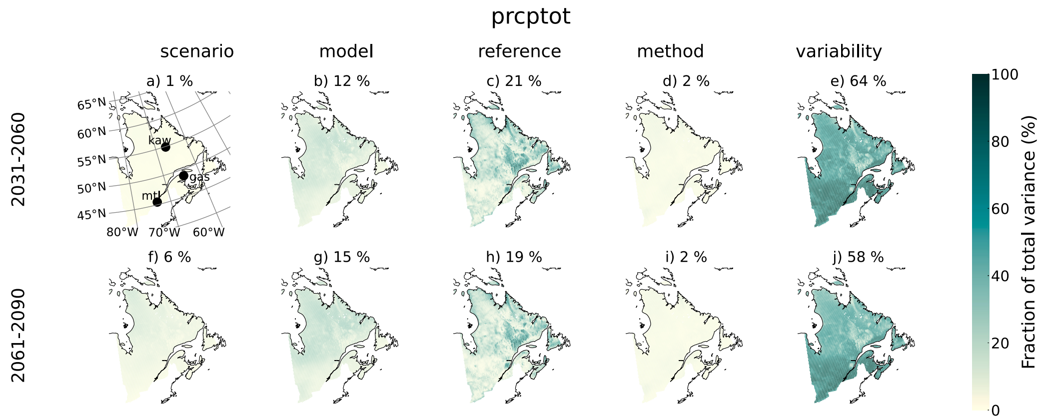

Fig. 4. Partitioning of uncertainty in total precipitation over eastern Canada for two 30-year periods.

$$U_r(t) = \sum_{g,s,m} w_{g,s,m} \mathrm{var}_r[\hat{x}(g, s, m, r, t)], \tag{8}$$

where w are the weights,

$$w_{g,s,m} = \frac{r_{g,s,m}}{\sum_{g,s,m} r_{g,s,m}}, \tag{9}$$

where $r_{g,s,m}$ is the number of references available for a given model, scenario, and method.

3. Results

This section presents the partition of uncertainty over time in three locations: Montréal (mtl), Gaspé (gas) and Kawawachikamach (kaw). These locations were chosen to represent different climates, observation station densities and environments (inland vs. coastal). Furthermore, we extend our analysis to encompass eastern Canada by illustrating each category of uncertainty over a 30-year period. Although only a subset of indicators is presented in this way, the rest of the indicators can be found in the supplemental figures (Fig. S11 to S16).

3.1. Precipitation

Fig. 3 shows the partitioning of total uncertainty into contributions from each component for precipitation indicators at the three aforementioned locations. Consistent with LS23, the largest share of the total variance is generally associated with interannual variability (dark green), with values ranging from 19% to 88%, depending on the location and indicator. It is the most important for the total precipitation.

The second largest source of uncertainty is generally associated with the observational reference (light teal), except for the number of dry days (bottom row) where it is the largest (more than half of total variance). The uncertainty associated with the models, scenarios and bias-adjustment methods is generally much lower than for the other two factors, combining for ~10% of the variance, except for the total precipitation over Kawawachikamach where they tend to be larger.

For the number of dry days (**dry_days**), the reference uncertainty is much larger than for other indicators. It should be noted that the number of dry days can vary widely between different observational datasets (Beck et al., 2017), and this is reflected in the wide spread between the different reference datasets (Fig. S1 j,k,l). LS23 also found that the number of dry days was the indicator for which the downscaling uncertainty (which included both reference and method) had the largest share.

The share of the variance associated with natural variability and the observational reference is generally consistent across the three locations and indicators, except for **prcptot** in Kawawachikamach and **r20 mm** in Montréal where the share of the variance associated with the reference tends to be larger. In both cases, the values of the indicator for CaSR v2.1, ERA5-Land and PCICBlend are usually close to each other, with EMDNA typically more of an outlier (S19 c and g). These results are similar when the constrained ensemble (with fewer models and scenarios) is evaluated (Fig. S8).

Fig. 4 shows the partition of the uncertainty for eastern Canada for two distinct 30-year periods. Unsurprisingly, we note that there is generally good agreement between areas where the fraction of the total variance associated with the reference is the largest and areas where there is greater disagreement between the four different references, as in Kawawachikamach (Fig. S5 a). We note that the pattern of increased variance over the area limited by Baie-Comeau/Fort Mackenzie/Havre-Saint-Pierre just north of the St. Lawrence River Estuary (centred around 52N, 65W) corresponds to the region where the precipitation is much higher in EMDNA than in the other references (not shown).

3.2. Temperature

For temperature indicators (Fig. 5), during the first half of the 21st century, much like precipitation indicators, the primary source of uncertainty is typically interannual variability. However, its share of the variance decreases over time as the uncertainty associated with the scenarios grows larger and becomes dominant. This result is similar to LS23, which showed a similar increase in the uncertainty associated with the emissions scenarios over time (LS23 Fig.2a). This is also expected with the inclusion of four different scenarios. With a constrained ensemble, including only the two more realistic scenarios, the models become the first source of uncertainty at the end of the century (Fig. S9). In both the constrained and complete ensembles, the uncertainty associated with the models is often the second largest in the first half of the century, except for **tx_max** in Gaspé and Kawawachikamach, where the reference uncertainty is more important. Generally, the third source of uncertainty is associated with the reference and is relatively constant over time, but can vary significantly across locations (see Fig. 6).

Both Gaspé and Kawawachikamach are located in regions of Quebec with sparse station coverage (Fig. S17), which can lead to disagreements among the different reference datasets. For example, in Gaspé, the average difference of **tx_max** between *CaSR v2.1* and *EMDNA* in the historical period is ~3.3 °C (Fig. S2). In LS23, the significance of downscaling uncertainty increased notably in areas characterized by sparse observations and observational discrepancies, for example, in Lagos. This can also occur when certain features are present in some references but not in others. For example, reference datasets that represents lakes (*CaSR v2.1* and *ERA5-Land*) will have colder maximum temperatures above and around the lakes compared to datasets that do not (*EMDNA* and *PCICBlend*). It is thus important to recognize that biases are not spatially uniform in the reference dataset and that they vary across regions depending on observational density, local

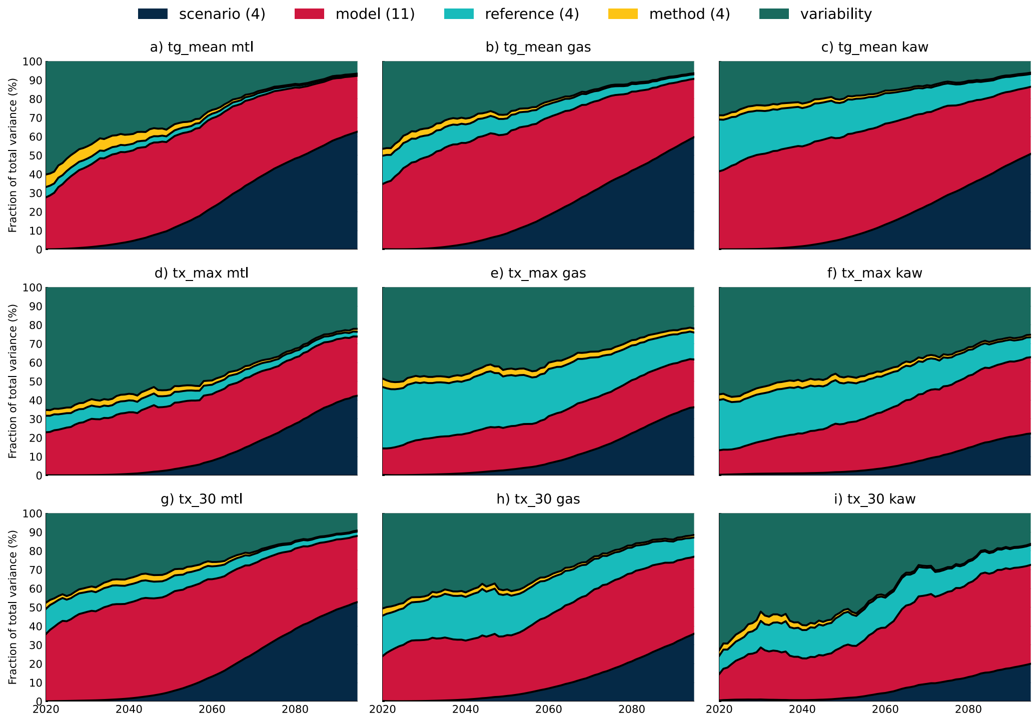

Fig. 5. Fraction of the total variance for temperature indicators over Montréal (mtl), Gaspé (gas) and Kawawachikamach (kaw).

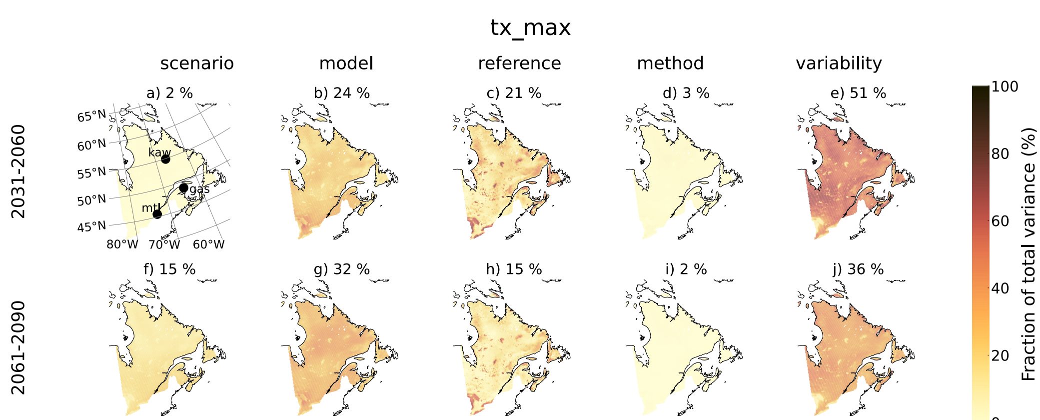

Fig. 6. Partitioning of uncertainty in maximum temperature over eastern Canada for two 30-year periods.

physiographic features, and the representation of those features in the reference datasets. As was the case with precipitation, the uncertainty associated with the bias-adjustment method remains small throughout the entire study period.

3.3. Multivariate indicators

Fig. 7 shows the partition of uncertainty for two multivariate indicators: the number of daily freeze-thaw cycles and the total amount of daily solid precipitation. The number of freeze-thaw cycles (**dlyfrzthw**) was chosen because it is an important indicator for climate change adaptation in northern countries (ClimateData.ca, 2025; US EPA, 2021). It combines both the maximum and minimum daily temperature and, as such, should be very sensitive to biases around the freezing point in the reference datasets. For this indicator, at the beginning of the century, the uncertainty associated with internal variability dominates near Montréal and Kawawachikamach, but the uncertainty associated with the observational reference largely dominates near Gaspé, being around twice that associated with the internal variability. In Gaspé, there is an average discrepancy of 45 days in the number of freeze-thaw cycles between the reference with the highest (*EMDNA*) and the lowest (*ERA5-Land*) number of occurrences (Fig. S3). This substantial difference could be explained by the fact that the maximum daily temperature and minimum daily temperature are not computed directly in *EMDNA*, but are derived from the daily mean and diurnal range. On Fig. S2 c, we can see that the mean temperature of EMDNA is very similar to the mean temperature of the other references. However, the daily minimum temperature (of EMDNA) is colder than all the other references while the daily maximum (of EMDNA) is warmer than all the other references (Fig. S4 b,e). In contrast, the daily minimum temperature in *ERA5-Land* is warmer than in the other references (Fig. S4 e). As freeze-thaw cycles are very sensitive to small changes in the distribution of temperatures near 0 °C , biases such as these can have a large impact on the number of cycles (Fig. S3 b).

We also note that, for freeze-thaw cycles, the choice of scenario has a negligible impact on the variance. This occurs because, with the warming of the climate, there is no detectable change in the

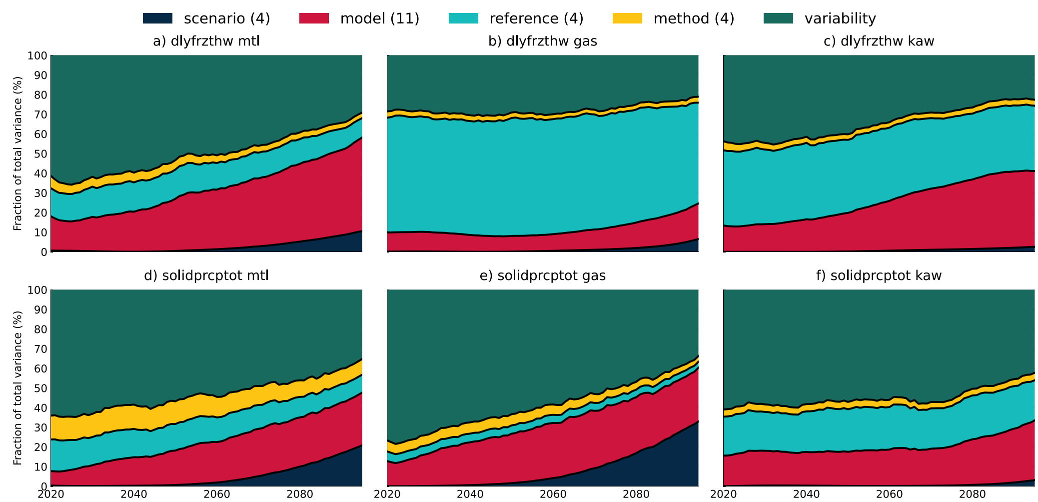

Fig. 7. Fraction of the total variance for multivariate indicators over Montréal (mtl), Gaspé (gas) and Kawawachikamach (kaw).

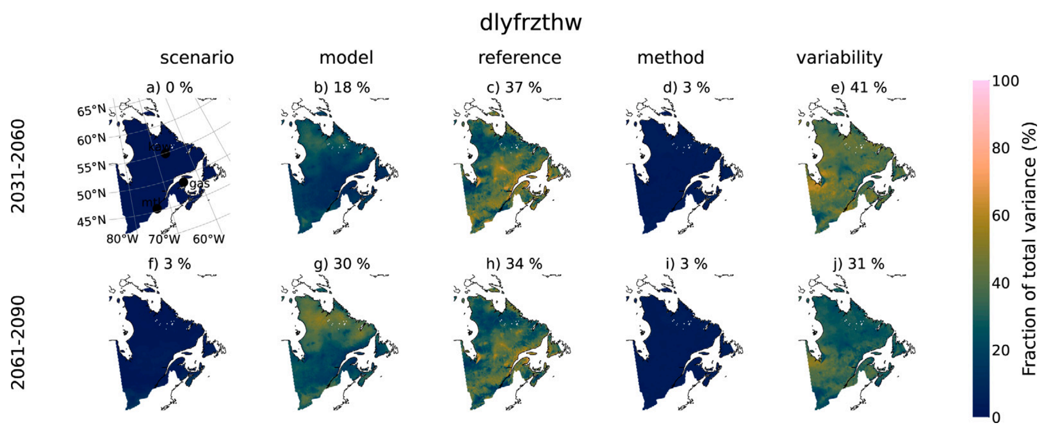

Fig. 8. Partitioning of uncertainty in number of freeze-thaw cycle over eastern Canada for two 30-year periods.

frequency of freeze-thaw cycles; rather, there is a temporal shift of these cycles from spring and fall into the winter months (Leduc and Logan, 2025). So we should not necessarily expect large differences between different emissions scenarios until the warming becomes so large that the number of cycles starts to decrease during the winter season.

The timing of the freeze-thaw season(s) also affects the spatial distribution. Fig. 8 shows that there is higher model uncertainty over the northern part of the province than over the southern part, especially near the end of the century. This is due to the fact that models do not agree on the sign of the change for **dlfrzthw** for that region. Over in the south, the models project either a decrease or no change, while in the north, they project a decrease or an increase (not shown). This may be because the projected warming could transform the one freeze-thaw season currently occurring in the summer into two seasons (similar to the southern part) of varying lengths in the spring and fall.

Fig. 8 shows significant spatial variability in the variance associated with the reference. In particular, we note higher values along the coast of the St-Lawrence River and Estuary and some areas north of 50°N. These areas with higher reference variance are co-located with the local maxima in variance associated with the reference in **tx_max**, which correspond to the locations of large lakes in northern Quebec. As with previous indicators, these areas are where we note the largest disagreement between the references (Fig. S7 a).

The estimated total amount of solid precipitation (**solidprcptot**) was selected as it combines the three variables that were adjusted here: minimum daily temperature, maximum daily temperature and total precipitation, as we consider that there is solid precipitation only when the mean temperature (derived from the maximum and minimum temperature) is below 0 °C . In this case, the uncertainty associated with the model is the largest (Fig. 7), second only to the uncertainty associated with the internal variability. It should be noted that the uncertainty associated with the bias-adjustment method reaches the highest value of any combination of location/indicator for the total amount of solid precipitation near Montréal (maximum of 13%). This variance is mainly introduced by `MBCn` (not shown), the only multivariate method used here. Fig. 9 shows that the methodology can represent an important fraction of the uncertainty in the south of the province, but less so in the north where temperatures remain below the freezing point for most of the year. In the latter case, the indicator **solidprcptot** is mainly dependent on precipitation rather than both near-surface temperature and precipitation.

4. Impact of the observational reference uncertainty in a decision-making context

The results from the previous section suggest that, in an ensemble of bias-adjusted climate simulations, there is generally more uncertainty associated with the observational reference than with the bias-adjustment methodology itself. Although the uncertainty associated with the models was larger than that associated with the reference for temperature-based indicators, this was not the case for precipitation-based indicators for which the reference was generally the second largest source of uncertainty after the interannual variability (or the first, in the case of the number of dry days).

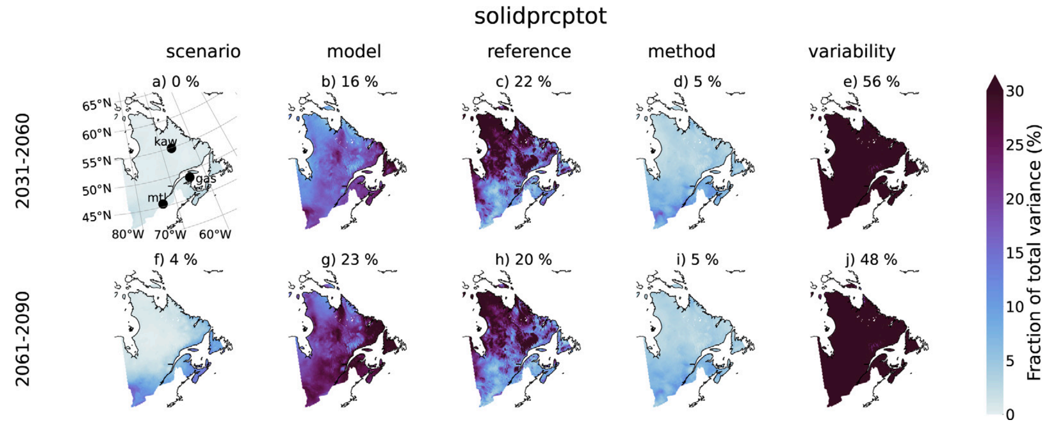

Fig. 9. Partitioning of uncertainty of solid precipitation over eastern Canada for two 30-year periods. Note that the colorbar is cut at 30% for better visualization.

We can examine the impact of this uncertainty through the lens of a climate service provider and three simple examples. In this section, as we are working with realistic examples, we use the constrained ensemble which is closer to an ensemble climate services might use for such adaptation projects. First, in August 2024, the remnants of Hurricane Debby broke the previous record of precipitation in Montréal by dropping 154 mm of rain on a single day over the city (Laframboise, 2024; Environment and Climate Change Canada, 0000). The storm caused widespread flooding over southern Quebec and became the costliest insured event in Quebec's history, even surpassing the 1998 ice storm (McCaffery, 2024). This event generated a great deal of media interest in regard to future precipitation and, in particular, the extent to which such extreme precipitation is likely to become more common due to climate change. Fig. 10c, shows the probability distribution for the maximum precipitation over a 24-h period (**rx1day**) for the different datasets for Montréal for the 2061–2090 period. We see that the extreme amount of rainfall that fell on Montréal that day would be outside the range projected by the ensemble bias adjusted using EMDNA and PCICBlend, which from a communication point of view is quite problematic. Note that we are showing data from a few stations to account for the different scale between a grid cell and a measurement at a station. More generally, the climate indicator **rx1day** is a climate indicator required for the climate adaptation plan of municipalities in Quebec (MELCCFP, 2024) and we can see that the distribution of that indicator for Montréal is significantly impacted by the reference dataset, potentially leading to costly maladaptation solutions to climate change. Another way to study extreme precipitation is to look at return periods. For example, if we look at the annual maximum daily precipitation for a return period of 20 years (Fig. S18), the difference between CaSR v2.1 and EMDNA is around 30 mm.

The second example highlights the impact of observational reference uncertainty in maximum temperatures on the safety assessment of welded railway tracks, as presented on climatedata.ca, the portal developed to support climate adaptation in Canada. In Canada, continuous welded rail tracks must be stress-tested during their installation. The historical value for this test across Canada has been 32.2 °C . This value is known as the preferred rail laying temperature (PRLT; Chiotti et al., 2017). The PRLT is usually chosen to be around the annual maximum temperature. If the track experiences temperatures significantly exceeding those during installation, this could result in the track bending or buckling (Zarembski, 1988). A train company participating in a climate change adaptation process might refer to a bias-adjusted dataset to determine whether the PRLT needs to be increased based on the projections of maximum air temperature. In Gaspé (Fig. 10a), they would get significantly different results depending on the dataset used as reference: an ensemble bias adjusted with EMDNA would find that the threshold is too low, an ensemble bias adjusted with CaSR v2.1 would suggest that the threshold will remain acceptable while an ensemble bias adjusted with ERA5-Land and PCIC-Blend will return an ambiguous result.

The third example addresses the dangers posed by slippery surfaces on train platforms, also presented on climatedata.ca. Daily freeze-thaw cycles are a hazard for passengers because the melting and refreezing of snow back into ice increases the likelihood of slips and falls. Hence, a transit authority that is renovating its infrastructure might consider using climate change projections of freeze-thaw cycles to decide whether or not to install heathers on their platforms. Unlike in the previous example, we cannot conclude unequivocally that the selection of the reference dataset for the bias adjustment would influence the decision because there is not a clear threshold for the decision. However, as noted in Section 3, the projections of freeze-thaw cycles for the end of the 21st century vary significantly between the 4 ensembles. Annual total freeze-thaw cycles over Gaspé differ by more than 40 days between the medians of EMDNA and ERA5-Land (Fig. 10 b). This magnitude of the difference is similar to the one found by Lavoie et al. (2024b) who examined the same phenomenon for the Greater Toronto Area. In that case, when comparing two different bias-adjusted climate datasets, the authors concluded that it would be possible to reach contrasting decisions due to dataset differences.

As these three examples suggest, the choice of reference data set for bias adjustment can play an important role in determining the outcome of a climate change adaptation strategy. This result raises questions on the robustness of the bias-adjusted climate projection disseminated through web platforms and the ethical responsibility of the data providers in communicating the associated uncertainty.

5. Conclusion

LS23 highlighted the risk of underestimating the uncertainty of bias-adjusted climate projections by neglecting the uncertainty associated with the bias-adjustment procedure. Their results suggest a very large uncertainty associated with this procedure, but their methodology did not allow them to isolate the uncertainty associated with the reference dataset used for the adjustment with the mathematical operation used to perform the adjustment. Here, by using a systematic approach that included four observational references and four bias-adjustment methods used operationally in Canada, we showed that, within this scope, the choice of the reference dataset tends to introduce more uncertainty than the bias-adjustment methodology used for adjusting the climate simulations.

We calculated the fraction of uncertainty associated with each dimension for precipitation, temperature and multivariate indicators over eastern Canada and focused particularly on three locations: Montréal, Gaspé and Kawawachikamach. We found that internal variability is usually the dominant uncertainty, especially near the present day. The

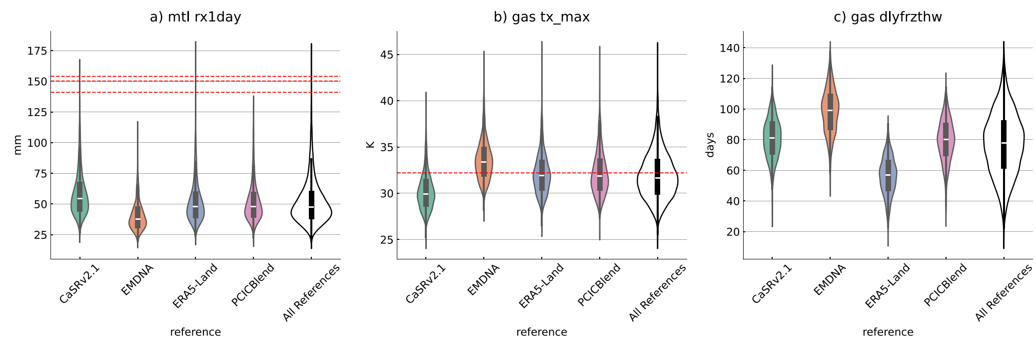

Fig. 10. Probability distribution for each reference based on all other dimensions (model, scenario, method) for the years 2061–2090. The boxplots in black show the quartiles of the dataset.

reference is usually the next most important uncertainty for precipitation indicators. For temperature indicators, the share of the uncertainty associated with the reference tends to be smaller due to the larger share of the uncertainty associated with the scenarios and the models, but is nonetheless important for locations with fewer observations (usually 2nd or 3rd most important source of uncertainty, excluding the internal variability) and tends to be more important than the uncertainty associated with the methodology. For multivariate indicators, the dominant uncertainty depends on the indicators and the location, though we note that this is where the bias-adjustment method has the largest impact. This is consistent with results of Sobie et al. (2024) who found large differences between the methods for multivariate indicators. Hence, in cases where multivariate indices are important, considering the method more thoroughly could be beneficial, while bearing in mind that different methodologies will impact various statistical properties differently (Alavoine and Grenier, 2022). We also note that we restricted our analysis to methods that are operational in Canada; including additional bias-adjustment approaches that differ substantially from the ones presented here might lead to an increase in the fraction of the variance associated with the bias-adjustment methodology.

This has significant implication in a world of limited resources where one ought to balance the need to capture the full range of uncertainty with the computing resources available: by ignoring the uncertainty and the biases present in the observation-based dataset, one reduces the full range of plausible values of future climate indicators and can induce a false sense of confidence in the projections. This can have serious consequences for the users of these datasets, which will often use these ensembles to drive impact models (e.g., hydrological models) where severe impacts often depend on non-linear effects. While evaluating the impacts of the reference dataset on impact models driven by bias-adjusted climate simulations is beyond the scope of this study, we showed through simple examples that the choice of the reference dataset used for the bias-adjustment could lead to different conclusions in regards to the adaptation solution or possibly create confusion if the related uncertainty is not properly communicated.

Due to limitations in computing resources, our analysis was limited to a relatively small territory, so it is difficult to extrapolate our results to other areas of the globe, in particular to regions that have a different climate. However, we note that the density of observations over Canada is highly inhomogeneous, with a high concentration of stations near its southern border, where most of the population lives, and much fewer observations in the northern part of the country (Fig. S17). This is reflected in the uncertainty associated with the reference dataset, which tends to be larger further north where there are fewer stations. In this way, northern Canada is not unlike many other regions of the globe where observations are relatively limited, such as the Global South, and results obtained for Kawawachikamach might provide an indication of the level of uncertainty associated with the observational reference that should be expected for these regions.

While applying our findings to different regions of the globe poses a challenge, we can nonetheless identify certain conditions or certain indicators for which the uncertainty associated with the observational reference plays an important role:

- regions with few observations or for which there are disagreements in the historical record,
- areas around lakes or near the coasts (for temperature-based indicators),
- the number of freeze-thaw cycles,
- the number of dry days.

We note that the uncertainty introduced by the reference datasets is reducible by nature. The fraction of the total variance could technically decrease by reducing the biases in the different reference datasets by increasing the number of observations that go into the observational product or by improving the method by which that product is manufactured. It could also be done a posteriori by anchoring the dataset to independent local stations and spatially interpolating correction parameters. In fact, a number of recent studies have suggested adding a pre-processing step wherein the reference dataset is adjusted using station data (Cucchi et al., 2020; Niazkar et al., 2023; de Padua and Ahn, 2024; Garibay et al., 2021). The latter technique could be helpful in reducing the range of uncertainty created by the references for some regions rich in observations. However, we note that many of the station data available in Canada have already been used in constructing three out of the four references (*EMDNA*, *CaSR v2.1* and *PCICBlend*), and because data is very sparse over large part of the country (Fig. S17), the expected benefit of such technique in this case is not clear.

While the uncertainty introduced by the reference datasets is reducible, this is not necessarily the same for all sources of uncertainty. Indeed, as Parker (2013) explains, the natural variability is a type of ontic uncertainty, which will always be present regardless of the state of our knowledge. As we saw with the precipitation indicators, this can still represent a very large part of the uncertainty. Including multiple model members can address this often overlooked uncertainty in decision-ready ensembles. The four other dimensions that were examined (model, scenario, reference and method) are epistemic uncertainties, meaning that they come from a lack of knowledge that could technically be filled (Jebeile, 2024; Parker, 2013). Unfortunately, this knowledge is currently lacking, and climate services providers must accurately represent the current state of knowledge.

As mentioned in the Introduction, there are a growing number of web platforms providing bias-adjusted climate information to stakeholders. The results presented here suggest that neglecting the uncertainty associated with the observational reference excludes an important component of the uncertainty in bias-adjusted datasets, which could potentially lead to maladaptation. One solution worth exploring is the use of equally defensible reference datasets in the creation of these bias-adjusted ensembles, by making use of additional members of the EMDNA dataset for example. In some other instances, the additional complexity that increasing the number of references introduces to the projections could render it less interesting from a user perspective, making alternative solutions more suitable, such as an in-depth analysis for the choice of the single reference, possibly leading to choosing different references for different indicators and regions. What seems certain is that not taking this uncertainty into account will provide users with a misleading level of confidence in climate projections.

Code and data availability

Files containing the 9 indicators for the 14 bias-adjusted datasets used in the main paper are available in the Zenodo repository https://doi.org/10.5281/zenodo.14397866.

The input raw climate simulations can be accessed through ESGF MetaGrid (https://aims2.llnl.gov/search). The *CaSR v2.1* reference is available through CaSPAr (https://caspar-data.ca). The *ERA5-Land* reference is available through Copernicus Data Store (https://cds.climate.copernicus.eu/cdsapp#!/dataset/reanalysis-era5-land?tab=overview). The *EMDNA* reference is available through the Federated Research Data Repository (https://www.frdr-dfdr.ca/repo/dataset/4bb24ee2-73e1-43a8-a929-126d2eb2bfa3). The *PCICBlend* reference is available through the PCIC data portal (https://data.pacificclimate.org/portal/gridded_observations/map/). The code for `DQM` method is available at https://github.com/Ouranosinc/ESPO-G. The code for the `DQM-EV` method is available at https://github.com/Ouranosinc/info-crue-cmip6. The `MBCn` method is available through the `R` package "MBC" (https://cran.r-project.org/package=MBC;. The code for the MBCn-EMDNA dataset is available at https://github.com/Ouranosinc/info-crue-cmip6/tree/mbcn-narval. The `BCCAQv2` method is available through the `R` package "ClimDown" (https://github.com/pacificclimate/ClimDown). The code for the analysis of this paper is available at https://github.com/Ouranosinc/partition. It is based on the xscen (Rondeau-Genesse et al., 2025) and xclim (Bourgault et al., 2024) libraries.

CRediT authorship contribution statement

Juliette Lavoie: Writing – original draft, Software, Formal analysis, Data curation, Conceptualization. **Louis-Philippe Caron:** Writing – original draft, Supervision, Conceptualization. **Travis Logan:** Writing – review & editing, Supervision, Conceptualization. **Stephen Sobie:** Writing – review & editing, Data curation. **Richard Turcotte:** Writing – review & editing, Conceptualization. **Edouard Mailhot:** Writing – review & editing, Conceptualization. **Jasmine Pelletier-Dumont:** Writing – review & editing, Conceptualization.

Declaration of Generative AI and AI-assisted technologies in the writing process

During the preparation of this work the authors used Writefull and ChatGPT in order to make the writing clearer. After using this tool/service, the authors reviewed and edited the content as needed and take full responsibility for the content of the publication.

Declaration of competing interest

The authors declare that they have no known competing financial interests or personal relationships that could have appeared to influence the work reported in this paper.

Acknowledgements

We acknowledge the World Climate Research Program, which, through its Working Group on Coupled Modelling, coordinated and promoted CMIP6. We thank the climate modelling groups for producing and making available their model output, the Earth System Grid Federation (ESGF) for archiving the data and providing access, and the multiple funding agencies who support CMIP6 and ESGF. We acknowledge Environment and Climate Change Canada (*ECCC*) as the source of the *CaSR v2.1* dataset. We acknowledge Copernicus and ECMWF as the source of the *ERA5-Land* dataset. This project was funded by the Government of Quebec through the INFO-Crue research program (project 709120). This paper is part of the "Building Capacity to Use Climate Data in Decision-Making in Canada" project at the Computer Research Institute of Montreal (CRIM) with funding by Environment and Climate Change Canada.

Appendix A. Supplementary data

Supplementary material related to this article can be found online at https://doi.org/10.1016/j.cliser.2025.100619.

Data availability

The link to the data is available in the code and data availability section.

References

Alavoine, M., Grenier, P., 2022. The distinct problems of physical inconsistency and of multivariate bias involved in the statistical adjustment of climate simulations. Int. J. Climatol. 43 (3), 1211–1233. http://dx.doi.org/10.1002/joc.7878, URL https://onlinelibrary.wiley.com/doi/abs/10.1002/joc.7878. _eprint: https://onlinelibrary.wiley.com/doi/pdf/10.1002/joc.7878.

Beck, H.E., Vergopolan, N., Pan, M., Levizzani, V., van Dijk, A.I.J.M., Weedon, G.P., Brocca, L., Pappenberger, F., Huffman, G.J., Wood, E.F., 2017. Global-scale evaluation of 22 precipitation datasets using gauge observations and hydrological modeling. Hydrol. Earth Syst. Sci. 21 (12), 6201–6217. http://dx.doi.org/10.5194/hess-21-6201-2017, URL https://hess.copernicus.org/articles/21/6201/2017/hess-21-6201-2017.html. Publisher: Copernicus GmbH.

Bentsen, M., Oliviè, D.J.L., Seland, O., Toniazzo, T., Gjermundsen, A., Graff, L.S., Debernard, J.B., Gupta, A.K., He, Y., Kirkevåg, A., Schwinger, J., Tjiputra, J., Aas, K.S., Bethke, I., Fan, Y., Griesfeller, J., Grini, A., Guo, C., Ilicak, M., Karset, I.H.H., Landgren, O.A., Liakka, J., Moseid, K.O., Nummelin, A., Spensberger, C., Tang, H., Zhang, Z., Heinze, C., Iversen, T., Schulz, M., 2019. NCC NorESM2-MM model output prepared for CMIP6 ScenarioMIP. http://dx.doi.org/10.22033/ESGF/CMIP6.608.

Boucher, O., Denvil, S., Levavasseur, G., Cozic, A., Caubel, A., Foujols, M.A., Meurdesoif, Y., Cadule, P., Devilliers, M., Dupont, E., Lurton, T., 2019. IPSL IPSL-CM6A-LR model output prepared for CMIP6 ScenarioMIP. http://dx.doi.org/10.22033/ESGF/CMIP6.1532, URL https://doi.org/10.22033/ESGF/CMIP6.1532.

Bourgault, P., Huard, D., Smith, T.J., Logan, T., Aoun, A., Lavoie, J., Dupuis, E., Rondeau-Genesse, G., Gammon, S., Alegre, R., Barnes, C., Beaupré Laperrière, A., Biner, S., Caron, D., Ehbrecht, C., Fyke, J., Keel, T., Labonté, M.P., Lierhammer, L., Low, J.F., Quinn, J., Roy, P., Squire, D., Stephens, A., Tanguy, M., Whelan, C., Braun, M., Castro, D., Diez-Sierra, J., Lamarche, A., Wang, H.M., Lehner, S., 2024. xclim: xarray-based climate data analytics. http://dx.doi.org/10.5281/zenodo.14503627, URL https://zenodo.org/records/14503627.

Byun, Y.H., Lim, Y.J., Shim, S., Sung, H.M., Sun, M., Kim, J., Kim, B.H., Lee, J.H., Moon, H., 2019. NIMS-KMA KACE1.0-G model output prepared for CMIP6 ScenarioMIP. http://dx.doi.org/10.22033/ESGF/CMIP6.2242.

Cannon, A.J., 2018. Multivariate quantile mapping bias correction: an N-dimensional probability density function transform for climate model simulations of multiple variables. Clim. Dyn. 50 (1), 31–49. http://dx.doi.org/10.1007/s00382-017-3580-6.

Cannon, A.J., Sobie, S.R., Murdock, T.Q., 2015. Bias correction of GCM precipitation by quantile mapping: How well do methods preserve changes in quantiles and extremes? J. Clim. 28 (17), 6938–6959. http://dx.doi.org/10.1175/JCLI-D-14-00754.1, URL https://journals.ametsoc.org/view/journals/clim/28/17/jcli-d-14-00754.1.xml. Publisher: American Meteorological Society Section: Journal of Climate.

Chadwick, C., Gironás, J., González-Leiva, F., Aedo, S., 2023. Bias adjustment to preserve changes in variability: the unbiased mapping of GCM changes. Hydrol. Sci. J. 68 (8), 1184–1201. http://dx.doi.org/10.1080/02626667.2023.2201450, Publisher: Taylor & Francis _eprint.

Chiotti, Q., Chan, K., Gulecoglu, E., Belaieff, A., 2017. Planning for Resiliency: Toward a Corporate Climate Adaptation Plan. Technical Report, Metrolinx, URL https://assets.metrolinx.com/image/upload/v1663237658/Documents/Metrolinx/Planning_for_Resiliency_2017_EN_final.pdf.

ClimateData.ca, 2025. Transportation module overview. URL https://climatedata.ca/explore/sector/transportation/transportation-module-overview/,

Copernicus Climate Change Service, 2019. ERA5-Land hourly data from 1950 to present. http://dx.doi.org/10.24381/CDS.E2161BAC, URL https://cds.climate.copernicus.eu/doi/10.24381/cds.e2161bac.

Cucchi, M., Weedon, G.P., Amici, A., Bellouin, N., Lange, S., Müller Schmied, H., Hersbach, H., Buontempo, C., 2020. WFDE5: bias-adjusted ERA5 reanalysis data for impact studies. Earth Syst. Sci. Data 12 (3), 2097–2120. http://dx.doi.org/10.5194/essd-12-2097-2020, URL https://essd.copernicus.org/articles/12/2097/2020/. Publisher: Copernicus GmbH.

de Padua, V.M.N., Ahn, K.H., 2024. Toward the reliable use of reanalysis data as a reference for bias correction in climate models: A multivariate perspective. J. Hydrol. 644, 132102. http://dx.doi.org/10.1016/j.jhydrol.2024.132102, URL https://www.sciencedirect.com/science/article/pii/S0022169424014987.

EC-Earth Consortium, 2019. EC-earth-consortium EC-Earth3 model output prepared for CMIP6 ScenarioMIP. http://dx.doi.org/10.22033/ESGF/CMIP6.251.

Environment and Climate Change Canada, 0000. Daily data report for August 2024 - Climate - environment and climate change Canada. URL https://climat.meteo.gc.ca/climate_data/daily_data_e.html?hlyRange=2013-02-13%7C2024-10-31&dlyRange=2013-02-14%7C2024-10-30&mlyRange=%7C&StationID=51157&Prov=QC&urlExtension=_e.html&searchType=stnName&optLimit=yearRange&StartYear=2024&EndYear=2024&selRowPerPage=25&Line=0&searchMethod=contains&Month=8&Day=31&txtStationName=Montreal&timeframe=2&Year=2024.

Eyring, V., Bony, S., Meehl, G.A., Senior, C.A., Stevens, B., Stouffer, R.J., Taylor, K.E., 2016. Overview of the coupled model intercomparison project phase 6 (CMIP6) experimental design and organization. Geosci. Model. Dev. 9 (5), 1937–1958. http://dx.doi.org/10.5194/gmd-9-1937-2016, URL https://gmd.copernicus.org/articles/9/1937/2016/. Publisher: Copernicus GmbH.

Forster, P., Storelvmo, T., 2023. The earth's energy budget, climate feedbacks and climate sensitivity. In: Intergovernmental Panel on Climate Change (IPCC) (Ed.), Climate Change 2021 – the Physical Science Basis: Working Group I Contribution To the Sixth Assessment Report of the Intergovernmental Panel on Climate Change. Cambridge University Press, Cambridge, pp. 923–1054. http://dx.doi.org/10.1017/9781009157896.009, URL https://www.cambridge.org/core/books/climate-change-2021-the-physical-science-basis/earths-energy-budget-climate-feedbacks-and-climate-sensitivity/AE57C97E588FF3060C7C7E47DD4F3C6E.

Gampe, D., Schmid, J., Ludwig, R., 2019. Impact of reference dataset selection on RCM evaluation, bias correction, and resulting climate change signals of precipitation. J. Hydrometeorol. 20 (9), 1813–1828. http://dx.doi.org/10.1175/JHM-D-18-0108.1, URL https://journals.ametsoc.org/view/journals/hydr/20/9/jhm-d-18-0108_1.xml. Publisher: American Meteorological Society Section: Journal of Hydrometeorology.

Garibay, V.M., Gitau, M.W., Kiggundu, N., Moriasi, D., Mishili, F., 2021. Evaluation of reanalysis precipitation data and potential bias correction methods for use in data-scarce areas. Water Resour. Manag. 35 (5), 1587–1602. http://dx.doi.org/10.1007/s11269-021-02804-8.

Gasset, N., Fortin, V., Dimitrijevic, M., Carrera, M., Bilodeau, B., Muncaster, R., Gaborit, E., Roy, G., Pentcheva, N., Bulat, M., Wang, X., Pavlovic, R., Lespinas, F., Khedhaouiria, D., Mai, J., 2021. A 10 km North American precipitation and land-surface reanalysis based on the GEM atmospheric model. Hydrol. Earth Syst. Sci. 25 (9), 4917–4945. http://dx.doi.org/10.5194/hess-25-4917-2021, URL https://hess.copernicus.org/articles/25/4917/2021/. Publisher: Copernicus GmbH.

Gebrechorkos, S.H., Leyland, J., Dadson, S.J., Cohen, S., Slater, L., Wortmann, M., Ashworth, P.J., Bennett, G.L., Boothroyd, R., Cloke, H., Delorme, P., Griffith, H., Hardy, R., Hawker, L., McLelland, S., Neal, J., Nicholas, A., Tatem, A.J., Vahidi, E., Liu, Y., Sheffield, J., Parsons, D.R., Darby, S.E., 2023. Global scale evaluation of precipitation datasets for hydrological modelling. Hydrol. Earth Syst. Sci. Discuss. 1–33. http://dx.doi.org/10.5194/hess-2023-251, URL https://hess.copernicus.org/preprints/hess-2023-251/. Publisher: Copernicus GmbH.

Gillett, N.P., 2024. Halving of the uncertainty in projected warming over the past decade. Npj Clim. Atmospheric Sci. 7 (1), 146. http://dx.doi.org/10.1038/s41612-024-00693-3, URL https://www.nature.com/articles/s41612-024-00693-3. Publisher: Nature Publishing Group.

Good, P., Sellar, A., Tang, Y., Rumbold, S., Ellis, R., Kelley, D., Kuhlbrodt, T., Walton, J., 2019. MOHC UKESM1.0-LL model output prepared for CMIP6 ScenarioMIP. http://dx.doi.org/10.22033/ESGF/CMIP6.1567.

Guo, Q., Chen, J., Zhang, X., Shen, M., Chen, H., Guo, S., 2019. A new two-stage multivariate quantile mapping method for bias correcting climate model outputs. Clim. Dyn. 53 (5), 3603–3623. http://dx.doi.org/10.1007/s00382-019-04729-w.

Hausfather, Z., Marvel, K., Schmidt, G.A., Nielsen-Gammon, J.W., Zelinka, M., 2022. Climate simulations: recognize the 'hot model' problem. Nature 605 (7908), 26–29. http://dx.doi.org/10.1038/d41586-022-01192-2, URL https://www.nature.com/articles/d41586-022-01192-2. Bandiera_abtest: a Cg_type: Comment Publisher: Nature Publishing Group Subject_term: Climate change, Policy, Climate sciences.

Hausfather, Z., Peters, G.P., 2020. Emissions – the 'business as usual' story is misleading. Nature 577 (7792), 618–620. http://dx.doi.org/10.1038/d41586-020-00177-3, URL https://www.nature.com/articles/d41586-020-00177-3. Bandiera_abtest: a Cg_type: Comment Publisher: Nature Publishing Group Subject_term: Climate change, Climate sciences, Energy, Policy, Society.

Hawkins, E., Sutton, R., 2009. The potential to narrow uncertainty in regional climate predictions. Bull. Am. Meteorol. Soc. 90 (8), 1095–1108. http://dx.doi.org/10.1175/2009BAMS2607.1, URL https://journals.ametsoc.org/view/journals/bams/90/8/2009bams2607_1.xml. Publisher: American Meteorological Society Section: Bulletin of the American Meteorological Society.

Huard, D., Fyke, J., Capellán-Pérez, I., Matthews, H.D., Partanen, A.I., 2022. Estimating the likelihood of GHG concentration scenarios from probabilistic integrated assessment model simulations. Earth's Futur. 10 (10), http://dx.doi.org/10.1029/2022EF002715, e2022EF002715, URL https://onlinelibrary.wiley.com/doi/abs/10.1029/2022EF002715. _eprint: https://agupubs.onlinelibrary.wiley.com/doi/pdf/10.1029/2022EF002715.

Hunter, R.D., Meentemeyer, R.K., 2005. Climatologically aided mapping of daily precipitation and temperature. J. Appl. Meteorol. Clim. 44 (10), 1501–1510. http://dx.doi.org/10.1175/JAM2295.1, URL https://journals.ametsoc.org/view/journals/apme/44/10/jam2295.1.xml. Publisher: American Meteorological Society Section: Journal of Applied Meteorology and Climatology.

Iizumi, T., Takikawa, H., Hirabayashi, Y., Hanasaki, N., Nishimori, M., 2017. Contributions of different bias-correction methods and reference meteorological forcing data sets to uncertainty in projected temperature and precipitation extremes. J. Geophys. Res.: Atmospheres 122 (15), 7800–7819. http://dx.doi.org/10.1002/2017JD026613, URL https://onlinelibrary.wiley.com/doi/abs/10.1002/2017JD026613. _eprint: https://onlinelibrary.wiley.com/doi/pdf/10.1002/2017JD026613.

Jebeile, J., 2024. From regional climate models to usable information. Clim. Change 177 (3), 53. http://dx.doi.org/10.1007/s10584-024-03693-7.

Lafferty, D.C., Sriver, R.L., 2023. Downscaling and bias-correction contribute considerable uncertainty to local climate projections in CMIP6. Npj Clim. Atmospheric Sci. 6 (1), 1–13. http://dx.doi.org/10.1038/s41612-023-00486-0, URL https://www.nature.com/articles/s41612-023-00486-0. Publisher: Nature Publishing Group.

Laframboise, K., 2024. Montreal drenched in record-breaking rain as tropical storm Debby's remnants hit Canada. Glob. News URL https://globalnews.ca/news/10692242/montreal-rain-record-tropical-storm-debby-eastern-canada/.

Lavoie, J., Bourgault, P., Smith, T.J., Logan, T., Leduc, M., Caron, L.P., Gammon, S., Braun, M., 2024a. An ensemble of bias-adjusted CMIP6 climate simulations based on a high-resolution North American reanalysis. Sci. Data 11 (1), 64. http://dx.doi.org/10.1038/s41597-023-02855-z, URL https://www.nature.com/articles/s41597-023-02855-z. Publisher: Nature Publishing Group.

Lavoie, J., Caron, L.P., Logan, T., Barrow, E., 2024b. Canadian climate data portals: A comparative analysis from a user perspective. Clim. Serv. 34, 100471. http://dx.doi.org/10.1016/j.cliser.2024.100471, URL https://www.sciencedirect.com/science/article/pii/S2405880724000268.

Leduc, M., Logan, T., 2025. The impact of climate change on the annual cycle of freeze-thaw events in eastern North America. J. Appl. Meteorol. Clim. -1 (aop), http://dx.doi.org/10.1175/JAMC-D-24-0190.1, URL https://journals.ametsoc.org/view/journals/apme/aop/JAMC-D-24-0190.1/JAMC-D-24-0190.1.xml. Publisher: American Meteorological Society Section: Journal of Applied Meteorology and Climatology.

Li, L., 2019. CAS FGOALS-g3 model output prepared for CMIP6 ScenarioMIP. http://dx.doi.org/10.22033/ESGF/CMIP6.2056.

Maraun, D., Widmann, M., Gutiérrez, J.M., Kotlarski, S., Chandler, R.E., Hertig, E., Wibig, J., Huth, R., Wilcke, R.A., 2015. VALUE: A framework to validate downscaling approaches for climate change studies. Earth's Futur. 3 (1), 1–14. http://dx.doi.org/10.1002/2014EF000259, URL https://onlinelibrary.wiley.com/doi/abs/10.1002/2014EF000259. _eprint: https://agupubs.onlinelibrary.wiley.com/doi/pdf/10.1002/2014EF000259.

Maurer, E.P., Hidalgo, H.G., 2008. Utility of daily vs. monthly large-scale climate data: an intercomparison of two statistical downscaling methods. Hydrol. Earth Syst. Sci. 12 (2), 551–563. http://dx.doi.org/10.5194/hess-12-551-2008, URL https://hess.copernicus.org/articles/12/551/2008/hess-12-551-2008.html. Publisher: Copernicus GmbH.

McCaffery, K., 2024. Hurricane Debby event is the costliest in Quebec's history. Insur. Portal URL https://insurance-portal.ca/article/hurricane-debby-event-is-the-costliest-in-quebecs-history/.

McKenney, D.W., Hutchinson, M.F., Papadopol, P., Lawrence, K., Pedlar, J., Campbell, K., Milewska, E., Hopkinson, R.F., Price, D., Owen, T., 2011. Customized spatial climate models for North America. Bull. Am. Meteorol. Soc. 92 (12), 1611–1622. http://dx.doi.org/10.1175/2011BAMS3132.1, URL https://journals.ametsoc.org/view/journals/bams/92/12/2011bams3132_1.xml. Publisher: American Meteorological Society Section: Bulletin of the American Meteorological Society.

Mearns, L.O., McGinnis, S., Korytina, D., Arritt, R., Biner, S., Bukovsky, M., Chang, H.I., Christensen, O., Herzmann, D., Jiao, Y., Kharin, S., Lazare, M., Nikulin, G., Qian, M., Scinocca, J., Winger, K., Castro, C., Frigon, A., Gutowski, W., 2017. The NA-CORDEX dataset. http://dx.doi.org/10.5065/D6SJ1JCH.

MELCCFP, 2024. Guide d'élaboration d'un plan climat. URL https://cdn-contenu.quebec.ca/cdn-contenu/adm/min/environnement/publications-adm/plan-economie-verte/programmes/accelerer-transition-locale/guide-elaboration-plan-climat.pdf.

Niazkar, M., Piraei, R., Menapace, A., Dhawan, P., Torre, D.D., Larcher, M., Righetti, M., 2023. Bias correction of ERA5-Land temperature data using standalone and ensemble machine learning models: a case of northern Italy. J. Water Clim. Chang. 15 (1), 271–283. http://dx.doi.org/10.2166/wcc.2023.669.

Ouranos, 2023. Scientific Guidelines to Facilitate the Use of Climate Projections. Technical Report Version 1, URL https://www.ouranos.ca/sites/default/files/2024-02/Scientific-guidelines-to-facilitate-the-use–of-climate-projections.pdf.

Parker, W.S., 2013. Ensemble modeling, uncertainty and robust predictions. WIREs Clim. Chang. 4 (3), 213–223. http://dx.doi.org/10.1002/wcc.220, URL https://onlinelibrary.wiley.com/doi/abs/10.1002/wcc.220. _eprint: https://wires.onlinelibrary.wiley.com/doi/pdf/10.1002/wcc.220.

Pierce, D.W., Cayan, D.R., Maurer, E.P., Abatzoglou, J.T., Hegewisch, K.C., 2015. Improved bias correction techniques for hydrological simulations of climate change. J. Hydrometeorol. 16 (6), 2421–2442. http://dx.doi.org/10.1175/JHM-D-14-0236.1, URL https://journals.ametsoc.org/view/journals/hydr/16/6/jhm-d-14-0236_1.xml. Publisher: American Meteorological Society Section: Journal of Hydrometeorology.

Rastogi, D., Kao, S.C., Ashfaq, M., 2022. How may the choice of downscaling techniques and meteorological reference observations affect future hydroclimate projections? Earth's Futur. 10 (8), http://dx.doi.org/10.1029/2022EF002734, e2022EF002734, URL https://onlinelibrary.wiley.com/doi/abs/10.1029/2022EF002734. _eprint: https://onlinelibrary.wiley.com/doi/pdf/10.1029/2022EF002734.

Rondeau-Genesse, G., Bourgault, P., Lavoie, J., Smith, T.J., Gammon, S., Logan, T., Caron, L.P., Braun, M., Bourdeau-Goulet, S.C., Gauvin St-Denis, B., Dupuis, E., 2025. Ouranosinc/xscen: v0.11.0. http://dx.doi.org/10.5281/zenodo.14726585, URL https://zenodo.org/records/14726585.

Roy, P., Rondeau-Genesse, G., Jalbert, J., Fournier, E., 2024. Climate scenarios of extreme precipitation using a combination of parametric and non-parametric bias correction methods in the province of Québec. Can. Water Resour. J. / Rev. Can. Ressources Hydriques 49 (1), 23–39. http://dx.doi.org/10.1080/07011784.2023.2220682, Publisher: Taylor & Francis _eprint: https://doi.org/10.1080/07011784.2023.2220682.

Shiogama, H., Abe, M., Tatebe, H., 2019. MIROC MIROC6 model output prepared for CMIP6 ScenarioMIP. http://dx.doi.org/10.22033/ESGF/CMIP6.898.

Sobie, S.R., Ouali, D., Curry, C.L., Zwiers, F.W., 2024. Multivariate Canadian downscaled climate scenarios for CMIP6 (CanDCS-M6). Geosci. Data J. n/a (n/a), http://dx.doi.org/10.1002/gdj3.257, URL https://onlinelibrary.wiley.com/doi/abs/10.1002/gdj3.257. _eprint: https://onlinelibrary.wiley.com/doi/pdf/10.1002/gdj3.257.

Sun, F., Mejia, A., Sharma, S., Zeng, P., Che, Y., 2020. Evaluating the credibility of downscaling: Integrating scale, trend, extreme, and climate event into a diagnostic framework. J. Appl. Meteorol. Clim. 59 (9), 1453–1467. http://dx.doi.org/10.1175/JAMC-D-20-0078.1, URL https://journals.ametsoc.org/view/journals/apme/59/9/jamcD200078.xml. Publisher: American Meteorological Society Section: Journal of Applied Meteorology and Climatology.

Swart, N.C., Cole, J.N.S., Kharin, V.V., Lazare, M., Scinocca, J.F., Gillett, N.P., Anstey, J., Arora, V., Christian, J.R., Jiao, Y., Lee, W.G., Majaess, F., Saenko, O.A., Seiler, C., Seinen, C., Shao, A., Solheim, L., von Salzen, K., Yang, D., Winter, B., Sigmond, M., 2019. CCCma CanESM5 model output prepared for CMIP6 ScenarioMIP. http://dx.doi.org/10.22033/ESGF/CMIP6.1317.

Switanek, M.B., Troch, P.A., Castro, C.L., Leuprecht, A., Chang, H.I., Mukherjee, R., Demaria, E.M.C., 2017. Scaled distribution mapping: a bias correction method that preserves raw climate model projected changes. Hydrol. Earth Syst. Sci. 21 (6), 2649–2666. http://dx.doi.org/10.5194/hess-21-2649-2017, URL https://hess.copernicus.org/articles/21/2649/2017/. Publisher: Copernicus GmbH.

Tang, G., Clark, M.P., Papalexiou, S.M., Newman, A.J., Wood, A.W., Brunet, D., Whitfield, P.H., 2021. EMDNA: an ensemble meteorological dataset for North America. Earth Syst. Sci. Data 13 (7), 3337–3362. http://dx.doi.org/10.5194/essd-13-3337-2021, URL https://essd.copernicus.org/articles/13/3337/2021/. Publisher: Copernicus GmbH.

US EPA, O., 2021. Climate Change Indicators: Freeze-Thaw Conditions. URL https://www.epa.gov/climate-indicators/climate-change-indicators-freeze-thaw-conditions.

Voldoire, A., 2019. CNRM-CERFACS CNRM-CM6-1 model output prepared for CMIP6 ScenarioMIP. http://dx.doi.org/10.22033/ESGF/CMIP6.1384.

Wang, X.L., Xu, H., Qian, B., Feng, Y., Mekis, E., 2017. Adjusted daily rainfall and snowfall data for Canada. Atmos.-Ocean 55 (3), 155–168. http://dx.doi.org/10.1080/07055900.2017.1342163, Publisher: Taylor & Francis _eprint.

Werner, A.T., Cannon, A.J., 2015. Hydrologic extremes – an intercomparison of multiple gridded statistical downscaling methods. http://dx.doi.org/10.5194/hessd-12-6179-2015, URL https://hess.copernicus.org/preprints/12/6179/2015/hessd-12-6179-2015.pdf.

Wootten, A.M., Dixon, K.W., Adams-Smith, D.J., McPherson, R.A., 2021. Statistically downscaled precipitation sensitivity to gridded observation data and downscaling technique. Int. J. Climatol. 41 (2), 980–1001. http://dx.doi.org/10.1002/joc.6716, URL https://rmets.onlinelibrary.wiley.com/doi/10.1002/joc.6716.

Yukimoto, S., Koshiro, T., Kawai, H., Oshima, N., Yoshida, K., Urakawa, S., Tsujino, H., Deushi, M., Tanaka, T., Hosaka, M., Yoshimura, H., Shindo, E., Mizuta, R., Ishii, M., Obata, A., Adachi, Y., 2019. MRI MRI-ESM2.0 model output prepared for CMIP6 ScenarioMIP. http://dx.doi.org/10.22033/ESGF/CMIP6.638.

Zarembski, A., 1988. Temperature and rail laying. Railw. Track Struct. URL https://www.rta.org/assets/docs/ComprehensiveRail/sec9/temperature%20and%20rail%20laying.pdf.

Ziehn, T., Chamberlain, M., Lenton, A., Law, R., Bodman, R., Dix, M., Wang, Y., Dobrohotoff, P., Srbinovsky, J., Stevens, L., Vohralik, P., Mackallah, C., Sullivan, A., O'Farrell, S., Druken, K., 2019. CSIRO ACCESS-ESM1.5 model output prepared for CMIP6 ScenarioMIP. http://dx.doi.org/10.22033/ESGF/CMIP6.2291.